ELSEVIER

Earth and Planetary Science Letters 148 (1997) 381–394

EPSL

Evaluating southern Red Sea corals as a proxy record for the Asian monsoon

R. Klein [a,d,*], A.W. Tudhope [a], C.P. Chilcott [a], J. Pätzold [b], Z. Abdulkarim [c], M. Fine [d], A.E. Fallick [e], Y. Loya [d]

[a] *Department of Geology and Geophysics, University of Edinburgh, Edinburgh, EH9 3JW, Scotland*
[b] *Fachberich Geowissenschaften, Universität Bremen, P.O. 330440, Bremen 28334, Germany*
[c] *Department of Biology, University of Asmara, P.O. Box 1220, Asmara, Eritrea*
[d] *Department of Zoology, Tel Aviv University, P.O.B. 39040, 69 978 Ramat Aviv, Israel*
[e] *Scottish Universities Research and Reactor Centre, East Kilbride, Glasgow G74 OQU, Scotland*

Received 21 May 1996; revised 23 January 1997; accepted 25 January 1997

Abstract

Coral palaeoclimatic studies are under way at many sites throughout the wet tropics. However, arid environments have received less attention. Here we report a high-resolution, 63 yr record of coral $\delta^{18}O$ and $\delta^{13}C$ extracted from a *Porites* colony from the Dahlak Archipelago, off the Eritrean coast, in the southern Red Sea. The annual cycles of the coral $\delta^{18}O$ and $\delta^{13}C$ are inversely related while their inter-annual variations show a strong positive correlation, with similar inter-decadal trends. Inter-annual variations in coral $\delta^{18}O$ show a relatively weak correlation with the southern Red Sea SST, but are strongly correlated with the Indian Ocean SST, especially on the decadal time-scale. The range of the inter-annual variations in the coral $\delta^{18}O$ is high compared to changes in local SST, due to the amplifying effect of simultaneous changes in water isotopic composition. Due to this amplification of the climate signal the coral provides a better indication of regional oceanographic behaviour than the local SST record. The norrtheast monsoon signal in the coral $\delta^{18}O$ dominates the mean annual signal and shows the best correlation with the instrumental data sets. It appears that variations in the coral $\delta^{18}O$ are controlled mainly by variations in the intensity of surface water influx from the Indian Ocean to the Red Sea during the winter northeast monsoon. Of particular significance is that the decadal time-scale variations in the coral skeletal $\delta^{18}O$ are closely correlated with both the Indian Ocean SST and with variations in the Pacific-based Southern Oscillation index. That is, isotopically light coral skeleton, indicating strong NE monsoon Red Sea inflow, correlates with periods of high Indian Ocean SST and with predominantly negative (El Niño) phases of the Southern Oscillation. The simultaneous nature of inter-decadal changes in Asian monsoon and ENSO behaviour suggest pan-Indo–Pacific tropical climate reorganisation and evolution.

Keywords: El Nino; paleoclimatology; O-18/O-16; Porites; Red Sea

* Corresponding author. Fax: +972 3 640 9403. Phone: +972 3 640 9809. E-mail: rklein@post.tau.ac.il.

PII S0012-821X(97)00021-6

1. Introduction

1.1. Corals as palaeoclimatic recorders

Massive corals can provide high resolution, multi-decadal palaeoclimatic records due to distinct annual banding in the physical structure and chemical composition of their skeletons [1–3]. These records can extend instrumental data sets, thereby revealing patterns of inter-annual or decadal timescale variability in the tropical climate system. In this context, the stable oxygen isotopic composition of the skeleton ($\delta^{18}O$) has proved to be of particular value.

Corals are known to precipitate their aragonitic skeleton out of oxygen isotopic equilibrium with ambient seawater (e.g., [4]) However, the offset from equilibrium appears to remain close to constant for individual coral genera. Consequently, the principal factors controlling variations in coral skeletal oxygen isotopic composition are changes in sea water temperature (approximately 0.21‰ decrease in skeletal $\delta^{18}O$ per 1°C rise in temperature [5]), and changes in seawater isotopic composition due to rainfall or evaporation [6]. Changes in growth rate exert an additional, but relatively minor control on skeletal $\delta^{18}O$ [4,7,8]. Therefore, depending upon the oceanographic setting, corals may yield reliable records of SST (where water composition remains close to constant), rainfall (where temperature remains close to constant), or some combination of the two [9–12]. Variations in coral $\delta^{13}C$ are more complex and difficult to interpret. They are generally related to changes in light intensity (through the activity of the coral symbiotic zooxanthellae that preferentially fix ^{12}C during photosynthesis) [13], changes in the isotopic composition of the dissolved bicarbonate in seawater or changes in the coral growth rate [4,14].

1.2. General characteristics of the study site

The Red Sea is a semi-enclosed silled basin separated from the Indian Ocean by narrow straits at Bab al Mandab (Fig. 1). The Dahlak Archipelago, situated at the southern end of the Red Sea off the coast of Eritrea, is about 130 km wide and 200 km long, and consists of hundreds of islands, most of which are surrounded by shallow shelf fringing reefs [15].

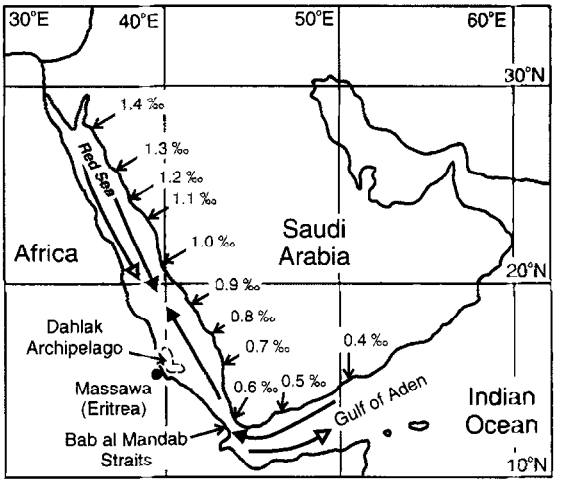

Fig. 1. A location map of the Red Sea and the northern Indian Ocean. Solid head arrows indicate the direction of surface winds during the winter NE monsoon season, and open head arrows, the direction of the surface winds during the summer SW monsoon season. Values in permil relate to the approximate $\delta^{18}O$ composition (SMOW) of surface water along a transect down the axis of the Red Sea and the central–southern Gulf of Aden in June 1984, interpolated from [19].

This part of the southern Red Sea is considered to be one of the hottest marine areas in the world, and the SST are among the highest reported for reef environments. Seasonal SST in the vicinity of Massawa range between a minimum of ~26°C in winter (January–February) and maximum of ~32°C in summer (August–September), and the average salinity is about 38‰. In general, cloud cover in this area is low throughout the year. The long-term mean rainfall, as measured in the vicinity of Massawa, is about 165 mm/yr (data provided by the Ministry of Marine Resources, Eritrea, for 1930–1990).

1.3. The Asian monsoon and circulation patterns

The hydrography and oceanography of the Red Sea are strongly influenced by the adjacent Indian Ocean through surface and subsurface circulation regimes, governed by the south Asian monsoon system and by thermohaline circulation [16–20]. The basic principles of the Asian monsoon system are that, during the summer, as a result of the differential sensible heating between land and ocean, there is formation of low atmospheric pressure over the Ti-

betan Plateau, and high atmospheric pressure above the relatively cold Indian Ocean at about 30°S. This results in a strong surface southwest airflow across the northern Indian Ocean. When the moist air from the ocean moves inland over the Indian subcontinent it causes heavy rain, known as the summer SW monsoon rainfall. During winter, rapid cooling over the Asian landmass results in a reversal of the temperature and atmospheric pressure gradients, resulting in dry northeast (NE) monsoon winds over the northern Indian Ocean region. The principle of the thermohaline circulation in the Red Sea is that the high evaporation rate, which exceeds the negligible amount of precipitation, increases the salinity, and consequently the density, of the surface water. The resulting pressure gradient creates net upper inflow of surface waters from the Indian Ocean towards the Red Sea and outflow of deep and dense Red Sea water in the opposite direction (e.g., [18]). As a result, during winter (November–April) the NE monsoon trade winds, together with thermohaline forces, create an inflow of surface waters from the Indian Ocean towards the southern Red Sea, while deep waters flow back out. During summer (May–October), the southwest (SW) monsoon winds and the thermohaline forces have opposite effects, resulting in a more complicated circulation regime, but with a pronounced net surface outflow towards the Indian Ocean. In addition, during winter the northern part of the Red Sea is affected by the north African wind system and northerly winds converge with the southerly winds at about 18–20°N [17] (Fig. 1). The physics controlling the nature of Red Sea circulation are now reasonably well understood and are reviewed by Eshel et al. [20], who successfully simulated the observed patterns using a linear box model.

1.4. The South Asian monsoon and the Southern Oscillation

It has long been recognised that variations in the intensity of the Asian and African monsoon show some degree of correlation with the Pacific El Niño Southern Oscillation (ENSO) (reviewed in [21]). The recurring large-scale climatic phenomenon ENSO describes an oscillation in sea level atmospheric pressure between the central Pacific and the north Australian/Indonesian region. The Tahiti–Darwin Southern Oscillation index (SOI), which is based on the standardised sea level pressure (SLP) between Tahiti (central Pacific) and Darwin (Australia), is a well defined measure for the state of the SO. Relatively low atmospheric pressure in the central Pacific and high pressure over Indonesia results in a negative value of the SOI and indicates the "warm" El Niño phase of the SO (the opposite pressure regime describes the "cold" La Niña phase of the oscillation). Previous studies have shown that years with above-average precipitation during the SW monsoon season over India, are often coincident with a high (positive) SOI, with low pressure and relatively warm temperatures over the Indonesian region and increased pressure and cool temperatures over the eastern Pacific Ocean, and vice versa in poor monsoon years [22,23]. Further evidence for atmospheric teleconnections that are associated with the extreme phases of the SO is shown by records of the Nile floods, where years of low Nile flood were associated with a low (negative) SOI [24].

1.5. The current study

Coral palaeoclimate records are now available from several climatically important localities in the tropics (e.g., Tarawa Atoll in the western-central equatorial Pacific [10], Galapagos Islands in the far eastern equatorial Pacific [11], and Papua New Guinea in the far western equatorial Pacific [25]). However, there are relatively few records from arid regions [26]. For this study, variations in the stable isotope composition ($\delta^{18}O$ and $\delta^{13}C$) of coral cores from the southern Red Sea were measured in order to assess their reliability as recorders of inter-annual/decadal climatic and oceanographic variability in this region, and to examine possible interactions with other climatic systems such as the south Asian (Indian Ocean) monsoon and the Pacific ENSO.

2. Material and methods

2.1. Sampling procedure and isotopic measurements

Coral cores were recovered from hemispherical *Porites* heads growing at depths between 4 and 6 m in the fringing reef attached to Dur-Ghella Island in

the Dahlak Archipelago. This small island is located about 50 km east of Massawa, in the western approach to Dahlak Kebir Island (15°43′N; 39°54′E). The cores, 5 cm in diameter, were drilled using an underwater pneumatic drilling machine connected to a low-pressure air compressor. Two cores, DGII and DGIII, recovered from two different colonies, ca. 0.5 km apart, are discussed in this paper. The cores were sectioned along their longitudinal axis to produce 6 mm thick slabs and X-rayed to reveal the annual density bands [27]. We subsampled continuously down the cores, parallel to growth direction, using a 3 mm diameter dental drill. Since the corals extended at rates of 15–20 mm/yr, this yielded 5–7 samples/annual growth increment. A long-term record of the $\delta^{18}O$ and $\delta^{13}C$ was extracted from core DGII, which represents 63 years (1931–1993). To permit an assessment of the reproducibility of this coral record, core DGIII (spanning the 34 year period 1960–1993) was subsampled and analysed at the same temporal resolution.

Oxygen and carbon stable isotope analyses were performed on 0.5–1.0 mg subsamples of carbonate powder. The coral powder was reacted with 100% orthophosphoric acid at 90°C in an automatic carbonate preparation line, and the resulting CO_2 gas was analysed on a VG Isogas Prism mass spectrometer (with a reproducibility (1σ) of $\pm 0.05‰$ for the $\delta^{13}C$ and $\pm 0.1‰$ for the $\delta^{18}O$ [28]). Results are reported in the conventional δ notation relative to the PDB isotopic standard. All the isotopic and chronology data are available as **EPSL Online Background dataset** [1] or, on request, from the senior author.

2.2. Data treatment

2.2.1. Skeletal $\delta^{18}O$ and climate records

Using the strong seasonal cycles present in the skeletal $\delta^{18}O$ record we developed a core chronology by designating the isotopically most negative sample in each year as August (the model month of highest SST). Linear interpolation between these minima was used to allocate a date to each intervening sample. In order to facilitate comparison of the coral $\delta^{18}O$ record with various climatic data, we calculated for each year, a mean annual value and seasonal values of the $\delta^{18}O$. To compute the seasonal records, we used the TIMER program (ARAND software, courtesy of P. Howell, Brown University), to develop records of 4 equal time steps per year, 3 months each (December–February, March–May, June–August, September–November), where the month intervals December–February and June–August represented the NE and SW monsoon seasons, respectively. Anomalies were computed by standardising the whole data to a 1951–1980 reference period (except for core DGIII, where data was normalised relative to the years 1960–1993). Annual mean anomalies were calculated for each of the four possible season combinations; that is: December–November, March–February, June–May, and September–August.

To permit examination of the relationships between coral skeletal $\delta^{18}O$ and local and regional SST, we compiled instrumental-based records of SST from the southern Red Sea and from a large area of the western tropical Indian Ocean. Specifically, we compiled the COADS SST record for the $2° \times 2°$ box centred on 15°N, 41°E (the closest marine box to the coral sampling site; data provided through NOAA, Boulder, Colorado), and a combined COADS and station-based record of the Indian Ocean region defined by 15°N–15°S, 55°E–75°E (data extracted from the World Climate Disc, Climatic Research Unit, University of East Anglia, 1992). The large geographical region selected for the Indian Ocean incorporates several major functional elements of Indian Ocean surface circulation and climate, and was chosen to give a first-order measure of inter-annual, regional-scale variations in low-latitude western Indian Ocean SST, rather than variations (temporal or spatial) in any single element of the system. The Tahiti–Darwin Southern Oscillation Index (T–D SOI, C.A.C version [29]) was used to give a measure of variations in the Pacific-based Southern Oscillation. In this index, negative anomalies are indicative of warm, El Niño, conditions, and positive anomalies of cool, La-Niña, conditions. Mean annual anomalies for SST and SOI records were computed relative to a 1951–1980 reference period, and for the same four possible season combinations as were computed for the coral $\delta^{18}O$ records.

[1] http://www.elsevier.nl/locate/epsl (mirror site USA, http://www.elsevier.com/locate/epsl)

In order to demonstrate the decadal and longer period variations in the coral and climatic data sets, visual comparison was made between data sets reduced to 5 yr mean values (i.e., 5 yr window; 5 yr step length between windows; n = 12 for a 60 yr record). Comparisons of all 5 possible year combinations were made to check on the robustness of the observed relationships. This indicated that the observed relationships are insensitive to movement of the 5 yr window.

2.2.2. Statistical procedures

Statistical relationships between the climatic and coral data sets were investigated through linear regression analysis and spectral analysis. First, linear regression analysis was performed on annual mean values. Analyses were performed for each of the four possible season combinations in order to ascertain which year boundaries yielded the best correlation between data sets. The highest correlations between coral $\delta^{18}O$ and the climatic data sets were found to be for the year defined as September–August, so this year is used throughout the rest of this paper. Comparisons were then made between data from specific seasons to help elucidate the nature and causes of relationships revealed in the annual data set analyses. Since the COADS SST record from the southern Red Sea contains missing data, regression analysis with this data set was limited to making comparisons once the periods of missing data had been removed from all records; that is, once the gaps in the record had effectively been closed.

In order to explore the relationships between the coral isotopic records and the climatic instrumental records in the frequency domain further, cross-spectral analysis was performed using the ARAND software (courtesy of Philip Howell, Brown University). Data sets at seasonal resolution were used. Since the Indian Ocean SST record displays a negative correlation with both coral $\delta^{18}O$ and T–D SOI, cross-spectral analysis was conducted using the negative SST time series to facilitate visual assessment of the phase relationships between records (i.e., to make the phase angle vary around 0° rather than around $+180/-180°$).

3. Results

3.1. Oxygen and carbon isotopes

3.1.1. Annual cycles

The high-resolution $\delta^{18}O$ and $\delta^{13}C$ profiles of core DGII are presented in Fig. 2. Both records display marked seasonality throughout the length of the 63 year records, with an annual amplitude of 0.4–1.2‰ for the oxygen (mean = 0.75‰) and 0.3–1.6‰ for the carbon (mean = 0.9‰). The annual $\delta^{18}O$ and $\delta^{13}C$ cycles are inversely correlated; isotopically light $\delta^{18}O$ coincides with heavy $\delta^{13}C$ and vice versa. We interpret this inverse relationship as being mainly due to increased photosynthesis during summer, which is in accordance with the isotope fractionation model suggested in [13]. By comparing

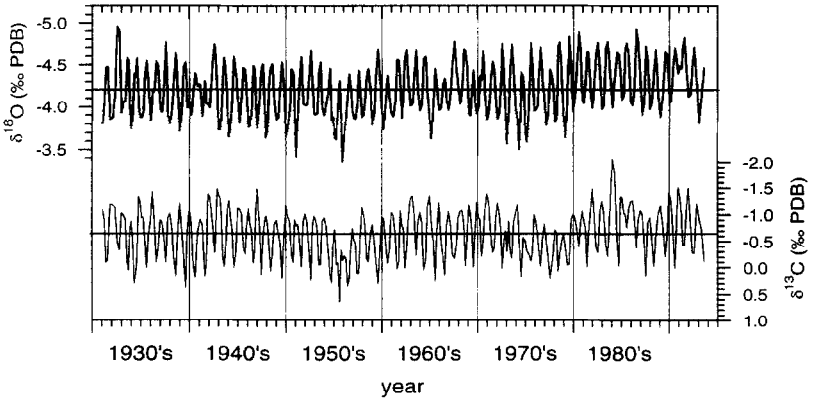

Fig. 2. The stable oxygen (upper line) and carbon (lower line) isotopic compositions of the 63 yr record (1931–1993) extracted from the coral core DGII. Horizontal lines are the mean values (−4.20‰ and −0.63‰ for $\delta^{18}O$ and $\delta^{13}C$, respectively).

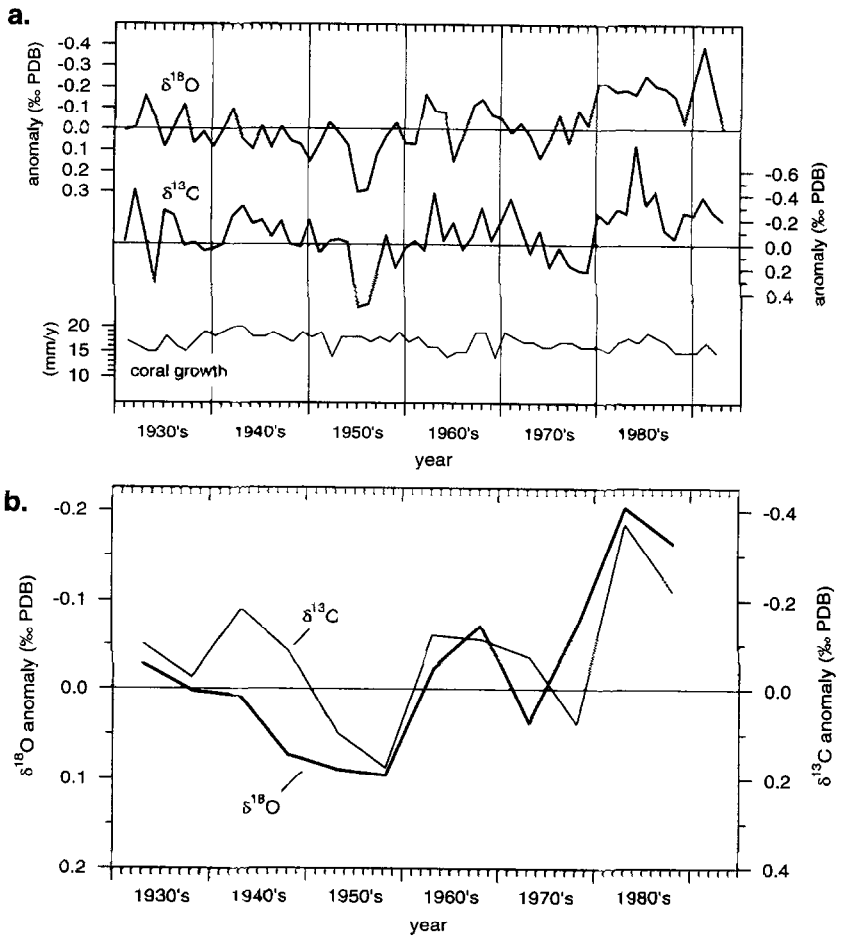

Fig. 3. (a) Mean annual anomalies (September–August) of $\delta^{18}O$ and $\delta^{13}C$ of coral DGII given in ‰ PDB plotted with the annual growth rate (linear extension). All mean annual values are plotted opposite the mid-point of the year. (b) 5 yr window means of coral DGII $\delta^{18}O$ and $\delta^{13}C$ plotted opposite the mid point of the 5 yr increments (anomalies given in ‰ PDB).

Table 1
Summary of the correlation coefficients (r values) between the coral isotopic records and the mean annual climatic records

Coral core DGII (1931–1993)	Annual means
Annual coral $\delta^{18}O$ vs. annual coral $\delta^{13}C$	0.53 [c] (n = 63)
Annual coral $\delta^{18}O$ vs. annual Indian Ocean SST	−0.68 [c] (n = 63)
Annual coral $\delta^{18}O$ vs. annual S. Red Sea SST	−0.33 [a] (n = 52)
Annual coral $\delta^{18}O$ vs. annual SO Index	0.37 [a] (n = 63)
NE monsoon coral $\delta^{18}O_{djf}$ vs. annual Indian Ocean SST	−0.61 [c] (n = 63)
NE monsoon coral $\delta^{18}O_{djf}$ vs. annual S. Red Sea SST	−0.45 [c] (n = 52)
NE monsoon coral $\delta^{18}O_{djf}$ vs. annual SO Index	0.50 [c] (n = 63)
SW monsoon coral $\delta^{18}O_{jja}$ vs. annual Indian Ocean SST	−0.45 [b] (n = 63)
SW monsoon coral $\delta^{18}O_{jja}$ vs. annual S. Red Sea SST	−0.07 ns (n = 52)
SW monsoon coral $\delta^{18}O_{jja}$ vs. annual SO Index	0.16 ns (n = 63)

All annual records were calculated from September to August.
[a] Significant at 95% level; [b] significant at 99% level; [c] significant at 99.9% level or greater; *ns* = not significant.

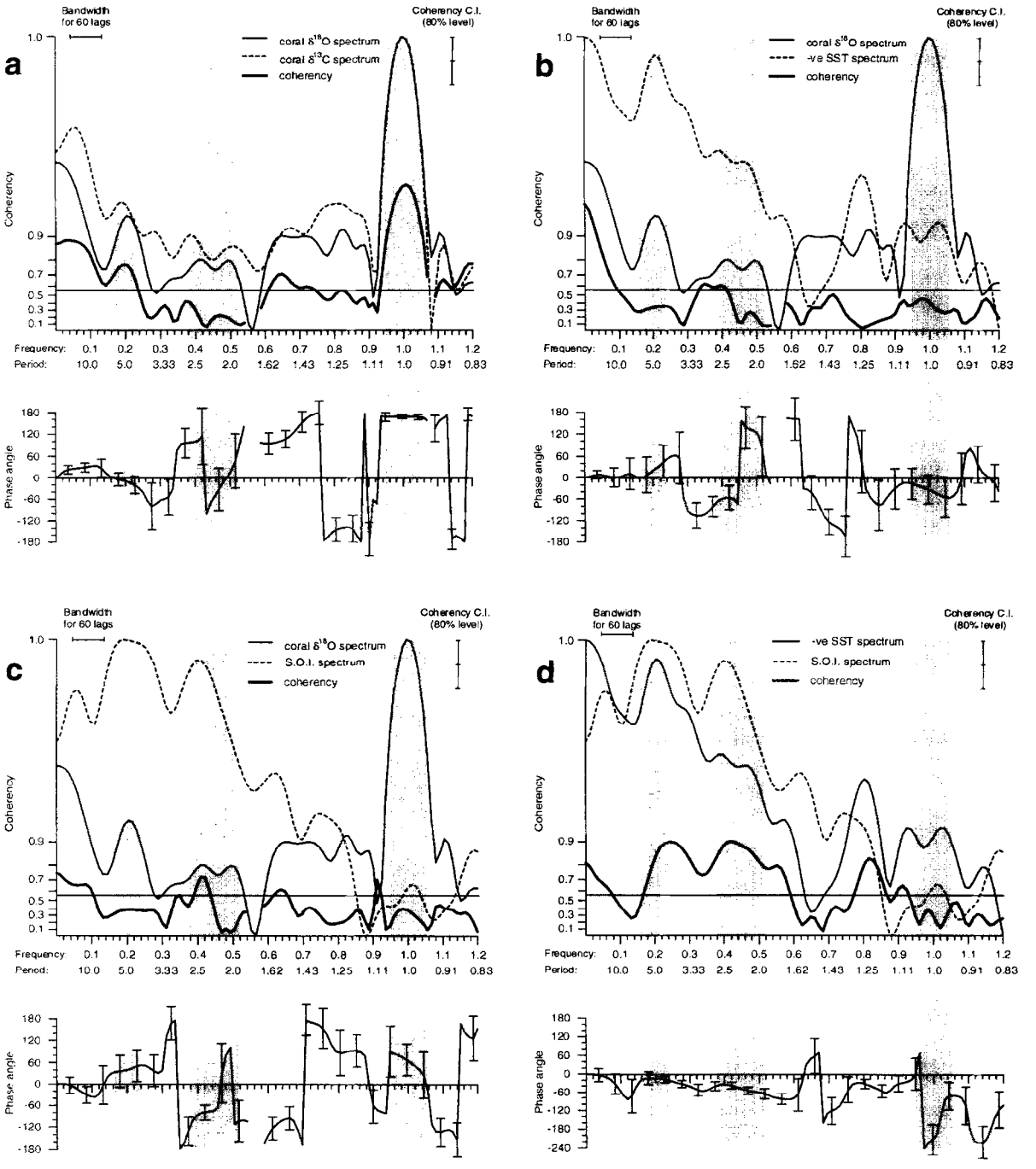

Fig. 4. Results of cross-spectral analysis for the period 1930–1990 using the ARAND software package with linear detrend of all records. (a) The coral $\delta^{18}O$ vs. $\delta^{13}C$. (b) The coral $\delta^{18}O$ vs. the negative Indian Ocean SST record. (c) The coral $\delta^{18}O$ vs. the T–D SOI record. (d) The SOI vs. the negative Indian Ocean SST record. The upper panel shows the concentration of variance as a function of frequency for the two parameters, and the coherency between the two records. The horizontal line indicates non-zero coherency confidence at the 80% level. The lower panel shows the phase angles. In each figure shading has been used to highlight periods centred on 1 yr, 2–2.5 yr and 5 yr.

the coral X-radiograph and the stable isotope records, we conclude that the high density bands have more negative $\delta^{18}O$ and more positive $\delta^{13}C$ compositions. Therefore, in these corals, seasonal high density bands appear to be deposited during periods when SST and sun irradiance are high (summer).

3.1.2. Inter-annual variability of the coral records

Annual mean values of $\delta^{18}O$ and $\delta^{13}C$ of core DGII are presented in Fig. 3a. The inter-annual variations in the $\delta^{18}O$ and $\delta^{13}C$ records are positively correlated (Table 1). Also plotted, to help reveal decadal trends, are the 5 yr mean values (Fig. 3b). Visual inspection of these isotopic records reveals the presence of two or three major inter-decadal cycles (ca. 20 yr each), in which periods of anomalously negative $\delta^{18}O$ coincide with periods of anomalously negative $\delta^{13}C$ and vice versa. Therefore, at the inter-annual and decadal time scales, skeletal $\delta^{18}O$ and $\delta^{13}C$ are positively correlated, whereas at the annual time scale they were negatively correlated. This interpretation is supported by the results of cross-spectral analysis between the $\delta^{18}O$ and $\delta^{13}C$ time series (Fig. 4a). A significant coherency between these records occurs at three variance peaks centred at 1 yr, 5 yr and at long periods (> 10 yr). Also, the two variables display concentrations of variance at about 2–2.5 yr but with low coherency. The strongest peak represents the annual cycle (1 yr periodicity) and the phase angle of 180° indicates an inverse relationship. The low phase angles for the 5 and > 10 yr peaks indicate that skeletal $\delta^{18}O$ and $\delta^{13}C$ are positively correlated.

Since coral growth rate is known to have an effect on isotopic compositions, inter-annual variations in the coral growth rate are presented in Fig. 3a (lower panel). This coral displays a high growth rate (linear extension) with an annual mean of 17 mm/yr. Although there are some visual similarities between the growth rate and the stable isotopic records (e.g., in the early 1940s, late 1960s and mid 1980s), linear regression analysis revealed no statistically significant correlation between the records, and, therefore, we suggest that changes in coral growth rate are not a major factor influencing the observed inter-annual isotopic variations.

3.2. Reproducibility of coral records

Original $\delta^{18}O$ time series and annual $\delta^{18}O$ means of the two coral cores (DGII and DGIII) for the period 1960–1993 are presented in Fig. 5. Although

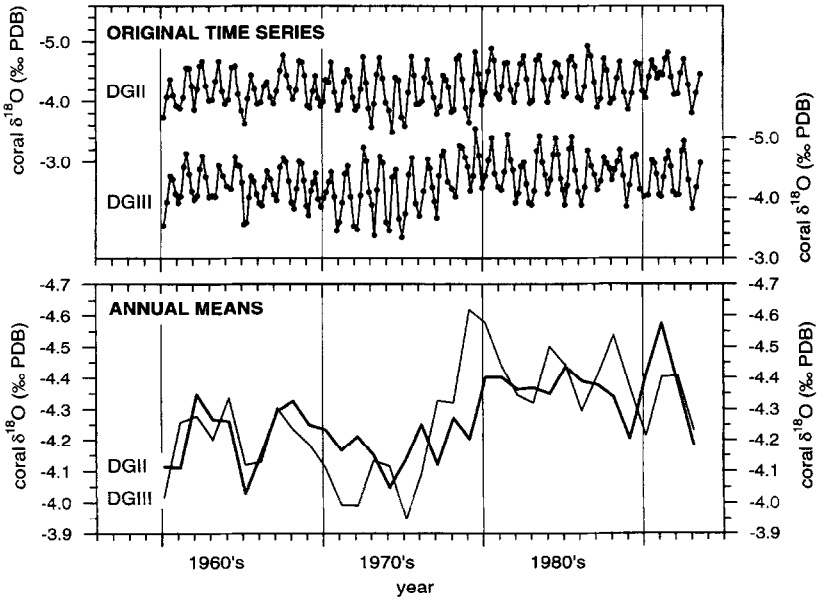

Fig. 5. $\delta^{18}O$ records from corals DGII and DGIII given in ‰ PDB. Top panel shows the original time series (5–7 samples/annual growth increment). Bottom panel shows the annual $\delta^{18}O$ means calculated for a year defined as September–August.

values for individual years are not always matched (top panel), the longer time-scale trends are similar in both records (bottom panel). A regression analysis between the two annual mean coral records yielded an r value of 0.56 ($p < 0.001$). The reason for differences between the isotopic records of the corals at the annual time-scale is unknown, but could conceivably be explained by differences in local environmental regimes (e.g., the direction of water currents, presence of nearby corals, etc.). However, at the seasonal resolution (4 samples/annual growth increment), both corals show similar $\delta^{18}O$ amplitudes (0.6‰ and 0.64‰ for corals DGII and DGIII, respectively). This observation implies that, in general, both corals respond similarly to the environmental signals.

3.3. Inter-annual variability of the coral oxygen isotopes and climatic data

Results of linear regression analysis between coral and climatic data sets are summarised in Table 1, and some of these relationships are illustrated visually as plots in Fig. 6. Fig. 4 presents the results of cross-spectral analysis. Annual mean coral $\delta^{18}O$ values are strongly correlated with the annual mean

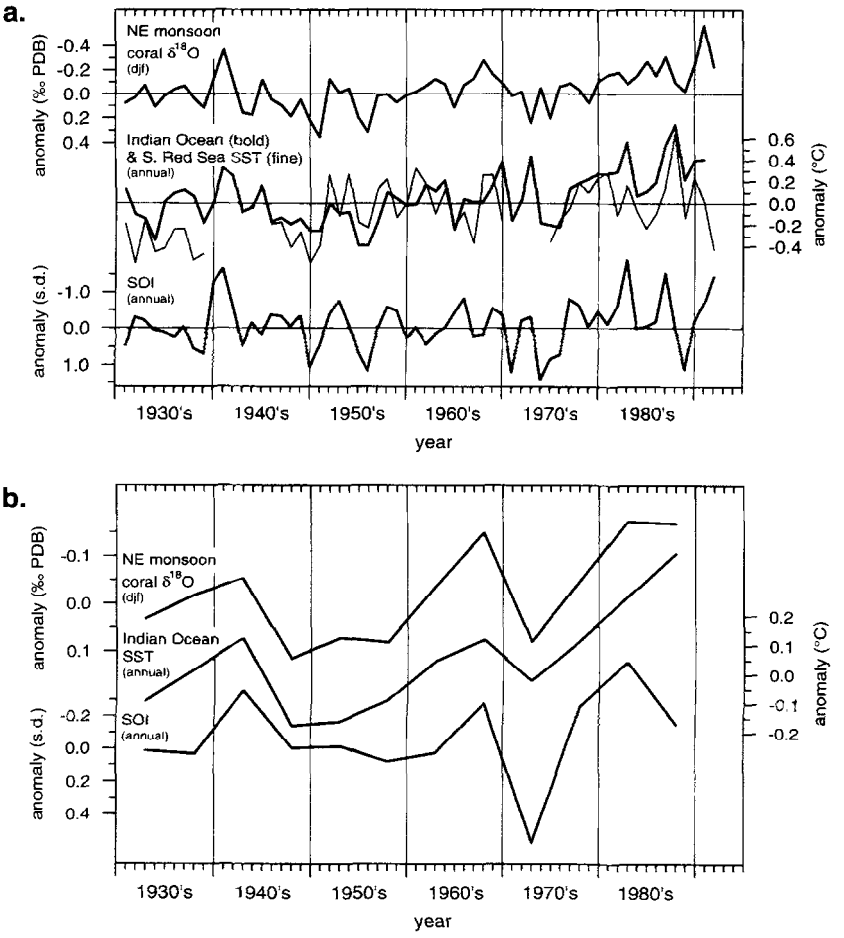

Fig. 6. (a) The NE monsoon coral $\delta^{18}O_{djf}$ anomalies of core DGII, plotted with mean annual (September–August) records of: Indian Ocean SST and southern Red Sea SST, and the T–D SOI. (b) Means of 5 yr window length, based on the annual records presented in (a). Data for the SOI is given in pressure anomalies (s.d. units). No 5 yr window means are presented for the non-continuous southern Red Sea SST record.

Indian Ocean SST values ($r = -0.68$, $p < 0.001$), and to a lesser, but still significant, extent with the annual mean SO Index and southern Red Sea SST data sets. These results indicate a tendency for deposition of isotopically light coral skeleton (negative anomalies) to coincide with elevated SST in the southern Red Sea and in the tropical western Indian Ocean, and with negative values of the SO Index. Visual comparison of 5 yr mean values (Fig. 6) reveals that the relationships between coral $\delta^{18}O$ and both Indian Ocean SST and the SO Index are still strong once variability less than the 5 yr period has been removed.

The technique of cross-spectral analysis allows further resolution of the nature of the relationships between the records as a function of frequency. The Indian Ocean SST and SOI records display coherent concentrations of variance for spectral peaks centred on about 4–5 yr, 2–2.5 yr and 1.25 yr (Fig. 4d). Although the 2–2.5 yr peak is weak in the case of the SST spectrum, these results imply that the area of the Indian Ocean selected for this study displays strong similarities to the SOI index across a range of typical ENSO frequencies. The coral $\delta^{18}O$ record also possesses concentrations of variance centred on around 5 yr and 2–2.5 yr, but these are not (5 yr period) or are only weakly (2–2.5 yr period) coherent with the Indian Ocean SST and SOI records (Fig. 4b,c). Although the lack of strong coherence implies that the coral oxygen record is not linearly related to either the Indian Ocean SST or SOI records at these periods, the presence of the spectral peaks does suggest that the coral $\delta^{18}O$ is influenced by ENSO-style dynamics. All 4 variables (coral $\delta^{18}O$, coral $\delta^{13}C$, SST and SOI) display coherent concentrations of variance at long periods (> 10 yr), and are close to being in phase (phase angle close to zero). Although these concentrations are poorly resolved by the spectral analysis technique (since the period is long with respect to the length of the time series), this result supports the conclusion that all the records share similar long-term trends.

Coral skeletal $\delta^{18}O$ for the NE monsoon season ($\delta^{18}O_{djf}$) is strongly correlated with mean annual values of all three instrumental data sets (Table 1 and Fig. 6). On the other hand, coral $\delta^{18}O$ for the SW monsoon season ($\delta^{18}O_{jja}$) is only weakly correlated with the mean annual Indian Ocean SST, and is not correlated with either the southern Red Sea SST or SO Index records. These results indicate that it is the NE monsoon signal in the coral skeletal $\delta^{18}O$ which dominates the mean annual signal, and that it is this signal which is best correlated with the instrumental data sets. The reasons for this relationship are discussed below.

4. Discussion

All the records discussed here (i.e., coral $\delta^{18}O$, coral $\delta^{13}C$, southern Red Sea SST, Indian Ocean SST, and SOI) show strong similarities in the pattern of decadal variability. This is also true when comparing the shorter isotopic profiles from the two cores DGII and DGIII. However, the year-to-year variations in all records match only in a few places along the 63 yr record, resulting in the relatively low (but highly significant) correlation coefficients when comparing annual mean values. In particular, the relationship between mean annual coral $\delta^{18}O$ and mean annual southern Red Sea SST is weak. Inter-annual variations in the annual mean southern Red Sea SST record are typically ca. 0.1–0.3°C (total range ca. 1°C; Fig. 6a), while variations in annual mean coral $\delta^{18}O$ record are typically around 0.1–0.3‰ (total range ca. 0.6‰, Fig. 3a). Since the temperature dependence relationship for aragonite precipitation from water is around 0.21‰/°C at 25°C [5], it may be concluded that the inter-annual SST variations observed in the COADS record are too small (by a factor of about 3) to account for the observed range of inter-annual coral $\delta^{18}O$ variations. This suggests that a significant proportion of the inter-annual signal in coral $\delta^{18}O$ may be the result of changes in seawater composition. The $\delta^{18}O$ (SMOW) of southern Red Sea waters is ca. 0.4‰ higher (heavier) than the Arabian Sea (northern Indian Ocean) waters, and ca. 0.6‰ lower (lighter) than the waters of the northern Red Sea (Fig. 1), as a consequence of differential evaporation [18,19]. Therefore, changes in directions and strengths of surface current flow into the southern Red Sea could result in changes in $\delta^{18}O$ of surface seawater in the area.

In order to further investigate the suggestion that variations in surface water $\delta^{18}O$ composition play a

major role in controlling the $\delta^{18}O$ of the coral skeleton, we compared the amplitudes of the annual cycle of the coral $\delta^{18}O$ and the Red Sea SST. Our sampling procedure of ca. 5–7 samples/annual growth increment did not allow us to capture the full magnitude of the annual coral $\delta^{18}O$ cycle. Nevertheless, the mean annual range of seasonal coral $\delta^{18}O$ (based on 4 samples/annual growth increment) was found to be 0.61‰, whereas the mean annual range of seasonal Red Sea SST was found to be 5.5°C for the period 1945–1992. Applying the usual temperature relationship [5], the expected coral $\delta^{18}O$ range was 1.16‰; that is, the observed coral $\delta^{18}O$ is approximately 50% of what would have been anticipated from consideration of the SST alone. These data imply that, over the seasonal cycle, changes in $\delta^{18}O$ composition of seawater and changes in SST may have opposing effects on coral skeletal $\delta^{18}O$.

We combined the observed relationships between all the isotopic and climatic records (Fig. 6) with the hydrographic and oceanographic features of the Red Sea, to suggest the following scenario: During the winter peak of the NE monsoon (December–February), the northeasterly trade winds promote increased surface water flow from the Indian Ocean into the Red Sea. As a consequence of the gradient in surface water $\delta^{18}O$ composition between the northern Red Sea and the western Indian Ocean (Fig. 1), this winter inflow will result in southern Red Sea surface waters becoming relatively light in oxygen isotopic composition compared to the summer SW monsoon condition. This seasonal change in southern Red Sea surface water $\delta^{18}O$ to lighter values occurs simultaneously to the annual SST minima, thereby explaining the observed reduced amplitude of the coral $\delta^{18}O$ annual cycle (see above). According to the physical principals of the monsoon system, an increase in the Indian Ocean SST would increase the land to sea temperature contrast in winter and, subsequently, the strength of the surface winds (see Section 1.3.). Therefore, warm SST anomalies in the equatorial Indian Ocean are expected to coincide with stronger than average NE monsoon winds. To investigate this idea further, the mean sea level pressure (MSLP) fields above India and the Red Sea during the NE monsoon months were examined (using the World Climate Disc, Climatic Research Unit, University of East Anglia, 1992). As predicted, we found that, in general, during periods of high Indian Ocean SST, there is a relatively steep gradient between the low MSLP trough above the Red Sea and the high MSLP ridge above India, and vice versa during periods of relatively low Indian Ocean SST. Therefore, we suggest that, during years of anomalously high SST in the low latitude western Indian ocean, the increased strength of the NE monsoon winds results in increased flow of surface waters into the Red Sea from the Arabian Sea. These Arabian

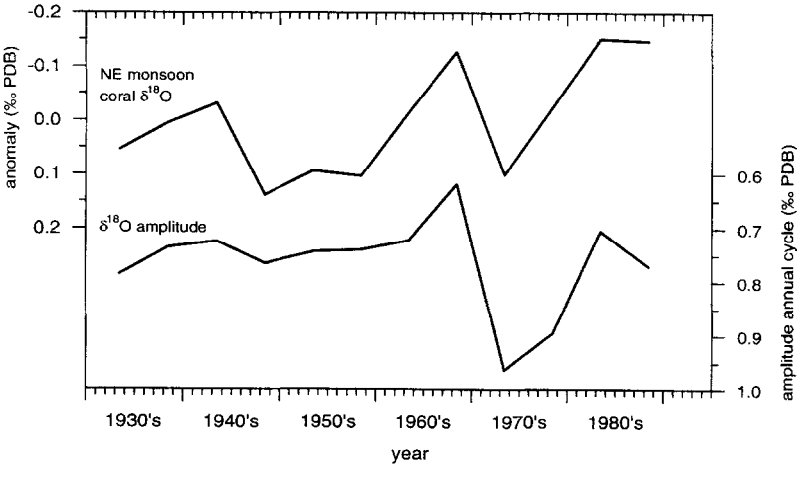

Fig. 7. 5 yr window means of the NE monsoon coral $\delta^{18}O_{djf}$ and the amplitude of the annual coral $\delta^{18}O$ cycles (computed as differences in permil between maximum and minimum isotopic values of each year in the original time series).

Sea waters are both warm and isotopically light with respect to oxygen compared to winter Red Sea surface waters. Therefore, although winter remains the season of coolest SST in the southern Red Sea, during years of anomalously strong NE monsoon winds this winter cooling is reduced, resulting in a relatively warm SST anomaly at the same time as an enhanced negative isotopic anomaly. This mechanism accounts for the "amplified" negative anomaly in coral skeletal $\delta^{18}O$ during the warm events. In addition, stronger than average winds during the NE monsoon period are likely to result in the northward displacement of the surface wind convergence zone (between NW winds over the northern Red Sea and SE winds over the southern Red Sea; Fig. 1), thereby reducing any contribution of cool, and isotopically heavy, northern Red Sea surface waters to the area of the Dahlak Archipelago. The correlation between the coral $\delta^{18}O_{djf}$ and the annual mean southern Red Sea SST, and the lack of correlation between the coral $\delta^{18}O_{jja}$ and the annual mean southern Red Sea SST record (Table 1) indicate that most of the inter-annual variability in the mean annual coral record is attributable to the variations taking place during the NE monsoon season. Further support for this conclusion comes from the pattern of variations in the amplitude of the annual $\delta^{18}O$ cycle along the 63 yr record. It appears that the amplitude tends to be lower during warm periods than during cool periods (Fig. 7). As discussed above, this indicates that, during warm periods, the negative annual $\delta^{18}O$ anomalies are primarily a reflection of a reduced winter "cooling" isotopic signal, a consequence of the enhanced winter influx to the southern Red Sea of relatively warm and isotopically light ($\delta^{18}O$) Indian Ocean water (and vice versa for the cool periods).

The coral $\delta^{18}O$ record provides a powerful proxy for regional oceanographic and climatological conditions due, in large part, to SST and water composition effects combining to induce a relatively high-amplitude inter-annual signal compared to the analytical errors (ca. ± 0.04‰ $\delta^{18}O$ 1σ for mean annual values based on 5–7 samples analysed). Inter-annual variations in the southern Red Sea SST on their own are relatively small. Indeed, the likely uncertainties surrounding the COADS annual SST estimates (possibly in the region of ± 0.1–0.2°C for small oceanographic areas such as the southern Red Sea; [30,31]) are close to the magnitude of the oceanographic "signal". That is, the instrumental SST record has an unfavourable signal:noise ratio for resolving the modes of the inter-annual climatic variations revealed by analysis of the coral. This factor may also explain, at least in part, the relatively weak correlation between the coral isotopic record and the instrumental SST record from the southern Red Sea.

We observed a strong inter-annual and inter-decadal correlation between the coral $\delta^{18}O$ and $\delta^{13}C$ (Fig. 3). This is well illustrated in the results of cross-spectral analyses of the two records (Fig. 4a). The lack of a significant correlation between these isotopic records and the annual growth rate in coral DGII (Fig. 3a) suggests that kinetic fractionation is not the cause of the $\delta^{13}C$ vs. $\delta^{18}O$ relationship. The $\delta^{13}C$ of the coral skeleton is modulated by variations in sunlight intensity and the isotopic composition of the ambient seawater. Since the cloud cover in this region is in general low [17], it seems unlikely that large variations in sunlight intensity (through changes in cloudiness) occurred simultaneously to the variations in SST and, if they occurred, they were probably not sufficient to induce large inter-annual changes such as 1‰ in the coral $\delta^{13}C$ (Fig. 3). Instead, it seems probable that the inter-annual changes in skeletal $\delta^{13}C$ reflect variations in the carbon isotopic composition of surface water in the region, or variation in the relative balance between heterotrophy and autotrophy in the coral metabolism. Without further information on spatial and temporal variation in surface water $\delta^{13}C$ it is not possible to differentiate between these possible causes. However, the coral $\delta^{13}C$ signal is clearly controlled by external environmental factors.

Finally, the decadal episodes of warming (or cooling) of the southern Red Sea surface waters, as extracted from the coral $\delta^{18}O$ record, occur simultaneously with phases of the negative (or positive) anomalies of the SOI, that represent El Niño (or La Niña) type conditions with increased (or decreased) SST in the eastern equatorial Pacific. For example, this can be clearly demonstrated for the early 1940s (Fig. 6a): 1940–1941 were identified as strong El Niño years, as seen from the negative anomalies of the SOI. During these years the SST of the Indian Ocean were anomalously high and manifested in the

anomalous negative values of the coral $\delta^{18}O_{djf}$. The opposite can be clearly demonstrated for the cold La Niña events in the early and mid 1950s. However, of the 14 recorded El Niño events between 1930 and 1987 [32], only 8 were manifested in our coral isotope record (Fig. 6a).

The relationship between the Pacific SO and the Indian Ocean SST is clearly demonstrated by the results of cross-spectral analysis (Fig. 4d). The two climatic/oceanographic systems are linked both at short and long time-scales, with a coherent concentration of variance at about 2–2.5, 5 and > 10 yr. Concentrations of variance at these periods are also recognised in the coral record. The highest coherency appears at the long period (> 10 yr). This indicates that the coral record provides a better proxy for the longer time-scale variability in these climate systems but still shows concentration of variance at shorter periods, of 2–6 yr, which are typical ENSO-style frequencies.

Although it is clear that there is a link between the south Asian monsoon and the Southern Oscillation [21–23], the mechanism of this interaction is not yet fully understood. Recent work indicates that the Indian Ocean possesses its own ENSO-style inter-annual variability [33]. Whether the ENSO signal in the Indian Ocean has a direct influence upon the ENSO signal in the Pacific Ocean (or vice versa) remains to be demonstrated. We suggest here that, on a decadal time-scale, there are simultaneous changes in the phases of the Southern Oscillation, the south Asian monsoon and the Indian Ocean SST, which are recorded in the stable isotope composition of the southern Red Sea corals. Such simultaneous changes provide further evidence for large-scale, pan-Indo–Pacific, reorganisation of atmosphere and surface ocean circulation patterns. The results of this paper also provide further evidence for the concept of global (or near global) inter-decadal climate oscillations (e.g., [34], and the utility of corals in investigating such phenomena.

5. Conclusions

In the present study, by using the stable isotopic composition of massive corals in the southern Red Sea, we: (1) provide a reliable and reproducible proxy record for the regional climate variability in the past 63 years, where instrumental records (e.g., SST) are discontinuous and of insufficient resolution to reveal the full environmental signal; (2) show that, over the annual cycle, changes in SST and surface water $\delta^{18}O$ work in opposite directions, resulting in a reduced coral skeletal $\delta^{18}O$ signal, whereas on the inter-annual timescale changes in SST and water isotopic composition combine to produce an amplified coral skeletal $\delta^{18}O$ climate signal; (3) show, by using a continuous data set of SST from a large oceanic area, that the variability in the coral record is linked to the variability in the climate of the surface tropical western Indian Ocean via circulation patterns; (4) suggest that this variability is mediated by the Asian monsoon system, especially during winter months (NE monsoon); and (5) by showing a correlation between the coral $\delta^{18}O$ and decadal variations in the El Niño Southern Oscillation, we provide further evidence for the longer period coupling of the Asian monsoon and ENSO systems, and hence demonstrate the potential of corals to contribute to our understanding of the operation of the Asian monsoon.

Acknowledgements

All isotopic measurements were carried out at the stable isotope laboratory at the SURRC, East Kilbride, Glasgow. We thank Mr. T. Donnelly from the SURRC for his technical advice and assistance. We also thank Phil Howell for supply of and advice with the use of the ARAND software package for spectral analysis, and Phil Jones for supply of climatic data. We express our gratitude to the Government of Eritrea, the Marine Resources Department (MRD), and the University of Asmara, for enabling us to perform the research project in the southern Red Sea. Special thanks are due to Dr. Chris Hillman from the MRD for his great assistance. The manuscript benefited significantly from the suggestions of the two reviewers, Dr. Dave Anderson and Dr. Dan Schrag. This work was supported by the German–Israeli Foundation for Scientific Research and Development (GIF), and grants from the British Council and the Harold Wingate Foundation. *[MK]*

References

[1] D.W. Knutson, R.W. Buddemeier and S.V. Smith, Coral chronometers: seasonal growth bands in reef corals, Science 177, 270–272, 1972.

[2] R.E. Dodge and J.R. Vaisnys, Hermatypic coral growth banding as environmental recorder, Nature 258, 706–708, 1975.

[3] R.W. Buddemeier, J.E. Maragos and D.W. Knutson, Radiographic studies of reef coral exo-skeletons: rates and patterns of coral growth, J. Explor. Mar. Biol. Ecol. 14, 179–200, 1974.

[4] T. McConnaughey, ^{13}C and ^{18}O isotopic disequilibrium in biological carbonates: I. Patterns, Geochim. Cosmochim. Acta 53, 151–162, 1989.

[5] S. Epstein, R. Buchsbaum, H.A. Lowenstam and H.C. Urey, Revised carbonate–water isotopic temperature scale, Bull. GSA 64, 1315–1325, 1953.

[6] P.K. Swart and M.L. Coleman, Isotopic data for scleractinian corals explain their palaeotemperature uncertainties, Nature 283, 557–559, 1983.

[7] L.S. Land, J.C. Lang and D.J. Barnes, Extension rate: A primary control on the isotopic composition of West Indian (Jamaican) scleractinian reef coral skeletons, Mar. Biol. 33, 221–233, 1975.

[8] N. Allison, A.W. Tudhope and A.E. Fallick, A study of the factors influencing the stable carbon and oxygen isotopic composition of *Porites lutea* coral skeletons, Phuket, South Thailand, Coral Reefs 15, 43–57, 1996.

[9] P. Aharon, Recorders of reef environment histories: stable isotopes in corals, giant clams, and calcareous algae, Coral Reefs 10, 71–90, 1991.

[10] J.E. Cole, R.G. Fairbanks and G.T. Shen, Recent variability in the Southern Oscillation: Isotopic results from a Tarawa Atoll coral, Science 260, 1790–1793, 1993.

[11] R.B. Dunbar, G.M. Wellington, M.W. Colgan and P.W. Glynn, Eastern Pacific sea surface temperature since 1600 A.D.: the $\delta^{18}O$ record of climate variability in Galapagos corals, Paleoceanography 9, 291–315, 1994.

[12] G.M. Wellington and R.B. Dunbar, Stable isotopic signature of El-Nino–Southern Oscillation events in eastern tropical Pacific reef corals, Coral Reefs 14, 5–25, 1995.

[13] J.N. Weber and P.M.J. Woodhead, Carbon and oxygen isotope fractionation in the skeletal carbonate of reef building corals, Chem. Geol. 6, 93–123, 1970.

[14] P.K. Swart, Carbon and oxygen isotope fractionation in scleractinian corals: a review, Earth Science Rev. 19, 51–80, 1983.

[15] O.H. Oren, Hydrography of Dahlak Archipelago (Red Sea), Sea Fish Res. Stat. Haifa Bull. 35, 3–22, 1962.

[16] S.A. Morcos, Physical and chemical oceanography of the Red Sea, Oceanogr. Mar. Biol. Annu. Rev. 8, 73–202, 1970.

[17] F.J. Edwards, Climate and oceanography of the Red Sea, in: Key Enviroments, Red Sea, A.J. Edwards and S.M. Head, eds., pp. 45–69, Pergamon, New York, NY, 1987.

[18] C. Mailard and G. Soliman, Hydrography of the Red Sea and exchanges with the Indian Ocean in summer, Oceanol. Acta 9 (3), 249–269, 1986.

[19] G. Ganssen and D. Kroon, Evidence for Red Sea surface circulation from oxygen isotopes of modern surface waters and planktonic foraminiferal tests, Paleoceanography 6 (1), 73–82, 1991.

[20] G. Eshel, M.A. Cane and M.B. Blumenthal, Modes of subsurface, intermediate, and deep water renewal in the Red Sea, J. Geophys. Res. 99, 15,941–15,952, 1994.

[21] H.F. Diaz and G.N. Kiladis, Atmospheric teleconnections associated with the extreme phases of the Southern Oscillation, in: El Niño, Historical and Paleoclimatic Aspects of the Southern Oscillation, H.F. Diaz and V. Markgraf, eds., pp. 7–28, Cambridge Univ. Press, Cambridge, 1992.

[22] B. Parthasarathy and G.B. Pant, Seasonal relationships between Indian summer monsoon rainfall and the Southern Oscillation, J. Climatol. 5, 369–378, 1985.

[23] U.S. Bhatt, Circulation regimes of rainfall anomalies in the African–South Asian monsoon belt, J. Climate 2, 1133–1144, 1989.

[24] W.H. Quinn, A study of Southern Oscillation-related climatic activity for A.D. 622–1900 incorporationg Nile River flood data, in: El Niño, Historical and Paleoclimatic Aspects of the Southern Oscillation, H.F. Diaz and V. Markgraf, eds., pp. 119–149, Cambridge Univ. Press, Cambridge, 1992.

[25] A.W. Tudhope, G.B. Shimmield, C.P. Chilcott, M. Jebb, A.E. Fallick and A.N. Dalgleish, Recent changes in climate in the far western equatorial Pacific and their relationship to the Southern Oscillation; oxygen isotope records from massive corals, Papua New Guinea, Earth Planet. Sci. Lett. 136, 575–590, 1995.

[26] G. Heiss, Coral reefs in the Red Sea: Growth, production, and stable isotopes, GEOMAR Rep. 32, 141 pp., 1994.

[27] R. Klein and Y. Loya, Skeletal growth and density patterns of two *Porites* corals from the Gulf of Eilat, Red Sea, Mar. Ecol. Prog. Ser. 77, 253–259, 1991.

[28] A.W. Tudhope, D.W. Lea, G.B. Shimmield, C.P. Chilcott and S. Head, Monsoon climate and Arabian Sea coastal upwelling recorded in massive corals from southern Oman, Palaios 11, 347–361, 1996.

[29] C.F. Ropelewski and P.D. Jones, An extension of the Tahiti–Darwin Southern Oscillation Index, Mon. Weather Rev. 115, 2161–2165, 1987.

[30] D.E. Parker, P.D. Jones, C.K. Folland and A. Beaven, Interdecadal changes of surface temperature since the late nineteenth century, J. Geophys. Res. 99, 14,373–14,399, 1994.

[31] K.E. Trenberth, J.R. Christy and J.W. Hurrell, Monitoring global monthly mean surface temperatures, J. Climate 5, 1405–1425, 1992.

[32] W.H. Quinn and V.T. Neal, The historical record of El-Niño events, in: Climate since A.D. 1500, R.S. Bradley and P.D. Jones, eds., pp. 623–648, 1992.

[33] Y.M. Tourre and W.B. White, ENSO signals in global upper ocean temperature, J. Phys. Ocean. 25, 1317–1332, 1995.

[34] M.E. Mann, J. Park and R.S Bradley, Global interdecadal and century-scale climate oscillations during the past five centuries, Nature 378, 266–270, 1995.